BJP British Journal of Pharmacology

DOI:10.1111/bph.12395
www.brjpharmacol.org

RESEARCH PAPER

Nicotinic receptor activation on primary sensory afferents modulates autorhythmicity in the mouse renal pelvis

M J Nguyen[1], S Angkawaijawa[1], H Hashitani[2] and R J Lang[1]

[1]*Department of Physiology, School of Biomedical Sciences, Monash University, Clayton, Vic., Australia, and* [2]*Department of Cell Physiology, Nagoya City University Graduate School of Medical Sciences, Nagoya, Japan*

Correspondence
Dr Richard J. Lang, Department of Physiology, Monash University, Wellington Road, Clayton 3800, Australia. E-mail: rick.lang@med.monash.edu.au

Keywords
nicotinic receptors primary sensory afferents; pyeloureteric peristalsis; smooth muscle, upper urinary tract

Received
21 April 2013
Revised
19 August 2013
Accepted
27 August 2013

BACKGROUND AND PURPOSE
The modulation of the spontaneous electrical and Ca^{2+} signals underlying pyeloureteric peristalsis upon nicotinic receptor activation located on primary sensory afferents (PSAs) was investigated in the mouse renal pelvis.

EXPERIMENTAL APPROACH
Contractile activity was followed using video microscopy, electrical and Ca^{2+} signals in typical and atypical smooth muscle cells (TSMCs and ASMCs) within the renal pelvis were recorded separately using intracellular microelectrodes and Fluo-4 Ca^{2+} imaging.

KEY RESULTS
Nicotine and carbachol (CCh; 1–100 μM) transiently reduced the frequency and increased the amplitude of spontaneous phasic contractions in a manner unaffected by muscarininc antagonists, 4-DAMP (1,1-dimethyl-4-diphenylacetoxypiperidinium iodide) and pirenzipine (10 nM) or L-NAME (L-Nω-nitroarginine methyl ester; 200 μM), inhibitor of NO synthesis, but blocked by the nicotinic antagonist, hexamethonium or capsaicin, depletor of PSA neuropeptides. These negative chronotropic and delayed positive inotropic effects of CCh on TSMC contractions, action potentials and Ca^{2+} transients were inhibited by glibenclamide (Glib; 1 μM), blocker of ATP-dependent K (KATP) channels. Nicotinic receptor-evoked inhibition of the spontaneous Ca^{2+} transients in ASMCs was prevented by capsaicin but not Glib. In contrast, the negative inotropic and chronotropic effects of the non-selective COX inhibitor indomethacin were not prevented by Glib.

CONCLUSIONS AND IMPLICATIONS
The negative chronotropic effect of nicotinic receptor activation results from the release of calcitonin gene-related peptide (CGRP) from PSAs, which suppresses Ca^{2+} signalling in ASMCs. PSA-released CGRP also evokes a transient hyperpolarization in TSMCs upon the opening of KATP channels, which reduces contraction propagation but promotes the recruitment of TSMC Ca^{2+} channels that underlie the delayed positive inotropic effects of CCh.

Abbreviations
$[Ca^{2+}]_i$, intracellular concentration of Ca^{2+}; 4-DAMP, 1,1-dimethyl-4-diphenylacetoxypiperidinium iodide; ASMC, atypical smooth muscle cell; CCh, carbachol; CGRP, calcitonin gene-related peptide; Dino, dinoprost; Glib, glibenclamide; hCGRP, human CGRP; Hex, hexamethonium; Indo, indomethacin; KATP, ATP-dependent K; L-NAME, L-Nω-nitroarginine methyl ester; M, muscarinic receptor; PSA, primary sensory afferents; PSS, physiological salt solution; STD, spontaneous transient depolarization; TSMC, typical smooth muscle cell

Introduction

The kidney has evolved to produce urine as a means of regulating a number of body homeostatic functions including the body's balance of ions, macronutrients, pH, osmotic concentrations, as well as controlling blood volume/pressure and removing toxic water-soluble compounds. In most small mammals, including the mouse, dog, cat, rat and rabbit, the kidney contains a single pyramid-shaped renal medulla, surrounded by a funnel-shaped calyx or renal pelvis. This renal pelvis consists of a urothelium-lined lumen and a plexus of bundles of long, spindle-shaped 'typical' smooth muscle cells (TSMCs), which form a continuous muscle layer, originating near the base of the papilla and extending through to the ureter (Gosling and Dixon, 1974; Klemm *et al.*, 1999).

Since the earliest examinations of kidney function, it has been recognized that the spontaneous propagating contractions that transport urine from the kidney to the bladder (pyeloureteric peristalsis) originate within the most proximal regions of the renal pelvis (Weiss *et al.*, 1967; Golenhofen and Hannappel, 1973). It is now well established that nifedipine-sensitive action potentials and Ca^{2+} waves within the TSMCs of the renal pelvis wall are responsible for the peristaltic contractions that propagate the length of the upper urinary system (Lang *et al.*, 2007a,b). In contraction-arrested preparations of renal pelvis (Klemm *et al.*, 1999; Lang *et al.*, 2001), spontaneous transient depolarizations (STDs) and Ca^{2+} transients are recorded in atypical SMCs (ASMCs), their discharge being dependent on the uptake and release of Ca^{2+} from internal stores (Lang *et al.*, 2007b). These STDs are thought to sum together to form the pacemaker signal that triggers the firing of the regenerative propagating action potentials (Lang, 2010; Lang *et al.*, 2010).

Even though there is evidence of extensive networks of parasympathetic and sympathetic nerves within the wall of the pelviureteric system (Rolle *et al.*, 2008), it has been difficult to demonstrate that these networks play any efferent role in maintaining or modulating pyeloureteric peristalsis. Spontaneous contractions in the pelviureteric system in human, guinea pig and rabbit are little affected by tetrodotoxin, N^G-nitro-L-arginine, guanethidine or atropine (Golenhofen and Hannappel, 1973; Maggi *et al.*, 1992; Lang *et al.*, 1998; Santicioli and Maggi, 1998). In the guinea pig and mouse renal pelvis, repetitive electrical nerve stimulation transiently reduces the frequency but increases the amplitude and duration of the spontaneous contractions (Santicioli and Maggi, 1998; Teele and Lang, 1998; Hashitani *et al.*, 2009). The positive inotropic effects have been attributed mostly to the release of excitatory tachykinins, substance P and neurokinin A from primary sensory afferents (PSAs), while the negative chronotropic effects have been associated with the release of calcitonin gene-related peptide (CGRP), a rise in cellular cAMP and a PKA-dependent activation of glibenclamide (Glib)-sensitive K^+ channels (Santicioli and Maggi, 1998; Hashitani *et al.*, 2009).

In this study, we investigated the effects of nicotinic receptor activation on the spontaneous contractions, action potentials and Ca^{2+} transients in TSMCs, as well as the Ca^{2+} transients in ASMCs of the mouse renal pelvis. The effects of nicotinic receptor activation were compared before and after neuropeptide depletion of PSAs or inhibition of ATP-dependent K^+ (KATP) channels, as well as with the effects of inhibition of PG synthesis. We propose that pre-synaptic PSA nicotinic receptors provide a means by which the extensive parasympathetic innervation in the renal pelvis can modulate pyeloureteric peristalsis.

Methods

All animal care and experimental protocols were in accordance with the National Health & Medical Research (Australia) guidelines and used procedures approved by the Animal Ethics Committees at Monash University and Nagoya City University. All studies involving animals are reported in accordance with the ARRIVE guidelines for reporting experiments involving animals (Kilkenny *et al.*, 2010; McGrath *et al.*, 2010). The total number of animals used in these experiments was 114. Male or female Swiss outbred or Balbc mice, 3–8 weeks in age were killed by cervical dislocation and exsanguination; the kidneys and attached ureters were removed through an abdominal incision.

Recording renal pelvic contraction and propagation

The renal pelvis of the mouse kidney attached to the parenchyma of a bisected kidney was dissected free of its surrounding fat and adventitia and pinned to the base of a recording chamber. The chamber was then mounted on a dissection microscope and washed (at 2 $mL \cdot min^{-1}$) with bicarbonate-buffered physiological salt solution (PSS) at 36°C. Changes in the diameter at 1 or 2 points on the renal pelvis were recorded with a video camera and analysed with edge detection software. Edge detection (Andor, Belfast, UK) of digital videos (at 25 frames per second) was sometimes also used to generate spatial temporal maps of the movement of the whole renal pelvis to quantify contraction propagation.

Intracellular microelectrode recordings

The upper urinary tract, from its point of attachment to the papilla to the pelviureteric junction, was dissected free of the kidney, opened along its longitudinal axis, pinned out in an organ bath, mounted on an inverted microscope and washed with warmed PSS (2 min^{-1}) as above. After 30 min equilibrium, preparations were observed to locate the region that displayed the most vigorous contractions. Longitudinal full-length strips (2× 10–20 mm^2) of the renal pelvis, including the most vigorous pacemaker region, were then cut and pinned firmly to the bottom of the organ bath. TSMCs were impaled using glass microelectrodes filled with 0.5 M KCl (tip resistance, 150–250 MΩ). Membrane potential changes were recorded with a high-input impedance amplifier (Axoclamp-2B, Axon Instruments, Inc., Foster City, CA, USA). After low-pass filtering (cut-off frequency, 2 kHz), membrane potential changes were digitized using a Digidata 1440A interface (Axon Instruments, Inc.) and stored on a personal computer for later analysis.

Measurements of intracellular Ca^{2+} concentration ($[Ca^{2+}]_i$)

To visualize changes in the $[Ca^{2+}]_i$ in ASMCs and TSMCs, preparations were pinned tightly with their serosal surface

uppermost to the Sylgard (Dow Corning Corporation, Midland, MI, USA) bottom of an organ bath and incubated with warmed (36°C) PSS, until spontaneous muscle contractions were observed. Preparations were then incubated in low-Ca^{2+} PSS ($[Ca^{2+}]_o$ = 0.1 mM) containing 1 μM Fluo-4 AM (Special packaging, Dojindo, Kumamoto, Japan) and cremophor EL (0.01%, Sigma, St Louis, MO, USA) for 30 min at 36°C and then 30 min at room temperature. After loading, the recording chamber was mounted on an inverted microscope (BX51, Olympus, Tokyo, Japan) equipped with an electron multiplier CCD camera (C9100 Hamamatsu Photonics, Hamamatsu City, Japan) and a high-speed scanning polychromatic light source (C7773 Hamamatsu Photonics). Preparations were viewed with a water immersion objective (UMPlanFI ×20 or LUMPlanFI ×60) and illuminated at 495 nm. Fluorescence emissions were captured through a barrier filter (above 515 nm) every 100–200 ms using AQUACOSMOS (Hamamatsu Photonics). Preparations were superfused (2 min^{-1}) with dye-free, warmed PSS (36°C) for 10–30 min. Relative changes in $[Ca^{2+}]_i$ were expressed as the ratio (F_t/F_0) of the fluorescence generated by an event at time (F_t) and the baseline fluorescence at t = 0 (F_0).

Solutions and drugs used

The PSS had the following composition (mM): NaCl 120, KCl 5, $CaCl_2$ 2.5, Mg SO_4 1–2, KH_2PO_4 1, $NaHCO_3$ 25 and glucose 11, bubbled with a 95% O_2: 5% CO_2 gas mixture to establish a pH of 7.3–7.4.

Drugs used were 4-DAMP (1,1-dimethyl-4-diphenylacetoxypiperidinium iodide), atropine, carbachol (CCh), dinoprost (Dino), forskolin, Glib, hexamethonium (Hex), IBMX, indomethacin (Indo), L-NAME (L-Nω-nitroarginine methyl ester), nicotine, PGE2, phenylephrine, pirenzepine, (from Sigma), capsaicin, tetrodotoxin (from Wako Pure Chemical Institute, Osaka, Japan) PCO400 (Santa Cruz Biotechnology, Dallas, TX, USA). Drugs were dissolved in distilled water, except for forskolin and Glib that were dissolved in dimethyl sulfoxide; capsaicin was dissolved in absolute ethanol. The final concentration of these solvents in the PSS did not exceed 1:1000.

Data analysis

The following parameters of spontaneous contractions, action potentials and Ca^{2+} transients were measured: peak amplitude measured from the resting level; half width, measured as the time between 50% peak amplitudes on the rising and falling phases; integral, the area under each event (integral) and frequency which was averaged over 2–3 min of recording. Variation between experiments was sometimes reduced by expressing the response in the presence of a drug (D) as a percentage change from control (C); that is, $100\times(D\text{-}C)\cdot C^{-1}$. Data is presented as the mean ± SEM, with n denoting the number of tissues. Paired or unpaired Student's t-tests were used as tests of significance; $P < 0.05$ was accepted as statistically significant (Lang *et al.*, 2007a,b).

All drug/molecular target nomenclature conforms to BJPs Guide to Receptors and Channels (Alexander *et al.*, 2011).

Results

Effects of nicotinic receptor activation

Spontaneous propagating contractions were observed in the mouse renal pelvis within 10–15 min equilibration. These contractions remained relatively consistent in frequency and amplitude for the following 3–4 h. Most preparations displayed propagating contractions that originated in the most proximal regions of the renal pelvis. However, some (<20%) preparations initially (first 10 min of equilibration) displayed contractions that arose from the distal renal pelvis. After 20 min, the origin of the spontaneous contractions in these preparations invariably switched to proximal regions of the renal pelvis (Davidson and Lang, 2000). Edge-detection monitoring at two points of known distance apart revealed propagating contractions had a mean amplitude (expressed as % of resting diameter), frequency and velocity of propagation of 9.8 ± 1%, 13.3 ± 1.6 min^{-1} and 1.2 ± 0.3 $mm\cdot s^{-1}$ (n = 13) respectively.

Table 1 summarizes the effects of four commonly used excitatory smooth muscle agonists on the spontaneous contractions of the mouse renal pelvis; 1 or 100 μM CCh, 1 or 100 μM phenylephrine, 10 nM PGE2 and 10 nM Dino, the stable analog of PGF2α. It can be seen that only Dino had a significant excitatory action on the renal pelvis (Figure 7Ai) and that PGE2 and phenylephrine (1 and 100 μM) were slightly, but not significantly excitatory. In contrast, CCh (1 μM) had no significant effects on renal pelvis contractility,

Table 1

Summary of the effects of four different smooth muscle agonists

	% Amplitude	% Frequency	% Velocity	*n*
1 μM CCh	–9.6 ± 7.0	3.56 ± 8.95	–27.1 ± 6.8[a]	6
100 μM CCh	6.2 ± 21.7	–57.0 ± 14.2[a]	–46.6 ± 13.4[a]	6
1 μM phenylephrine	24.7 ± 13.8	2.19 ± 7.36	6.2 ± 7.5	8
100 μM phenylephrine	73.7 ± 30.5	10.36 ± 38.4	–5.4 ± 14.9	8
10 μM PGE	1.7 ± 15.2	16.8 ± 16.9	47.6 ± 41.7	7
10 nM Dino	–12.4 ± 5.8	16.7 ± 7.7[a]	34.7 ± 17.1	15

Data expressed as % change from control and shown as mean ± SE of the mean.
[a]Denotes value significantly different from 0 ($P < 0.05$).

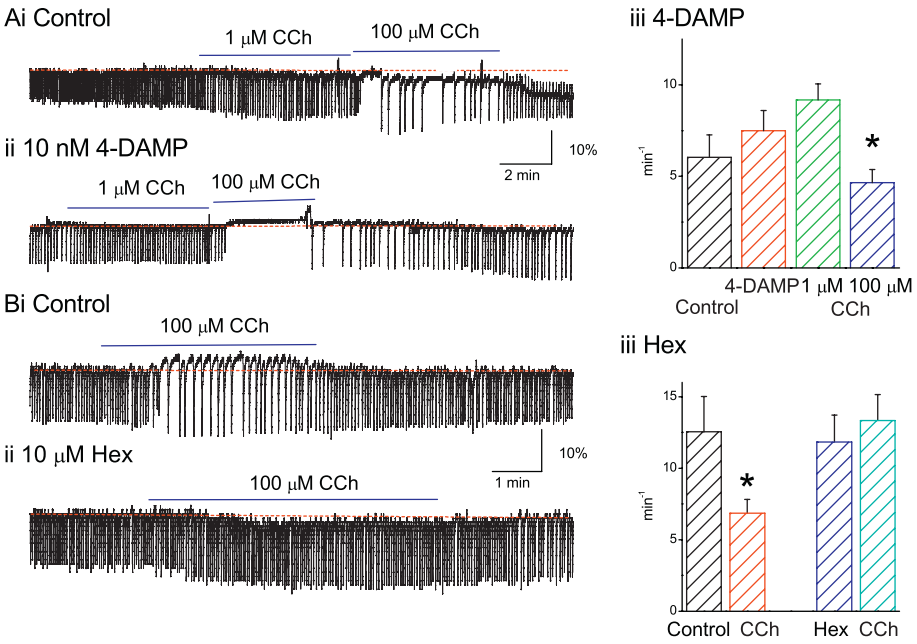

Figure 1

Effects of muscarinic and nicotinic antagonists on the negative chronotropic and positive inotropic actions of CCh (100 μM) on the spontaneous contractions in the mouse renal pelvis. Renal pelvis diameters were monitored at a single point using edge detection software, downward deflections represent a decrease in diameter expressed as a percentage of the resting diameter (dotted line). The significant decrease in frequency evoked by CCh (100 μM) was not prevented by the muscarinic antagonist 4-DAMP (10 nM, n = 4) (Ai–ii) but completely abolished by Hex (100 μM, n = 6) (Bi–ii). Results are summarized in Aiii and Biii; * denotes a significant difference from 4-DAMP in Aiii, and from control in Biii.

while CCh (100 μM) decreased the frequency (negative chronotropic effect) and propagation velocity of the spontaneous contractions, which remained for many minutes (>10 min) after washout.

Closer examination of the time course of the action of CCh (100 μM for 2–10 min) revealed that the negative chronotropic effect was often not maintained throughout the exposure period (Figure 1Bi). The initial decrease in frequency was often accompanied by an increase in the resting baseline diameter of 1–2%, which was followed by a transient increase in contraction amplitude (positive inotropic effect) as the baseline slowly returned to control levels.

To eliminate the involvement of urothelium-released NO, experiments were repeated in the presence of L-NAME (200 μM). After 30 min exposure to L-NAME, CCh (100 μM, n = 5) still evoked the transient negative chronotropic and delayed positive inotropic effects observed in control solutions (data not shown).

Effects of muscarinic (M) and nicotinic receptor antagonists

The effects of CCh (1 and 100 μM) were examined in the presence of a non-selective M antagonist, 4-DAMP (10 nM for 30 min, n = 4; Figure 1Ai-iii). As illustrated in Figure 1Ai–iii, the negative chronotropic effects of CCh were little affected by 4-DAMP. Similar results were obtained with the non-selective muscarinic antagonist, atropine (10 nM for 30 min, n = 2) and prenzipine (10 nM for 30 min, n = 3), a selective blocker of M1 and M4 Ms (data not shown).

The relatively high concentration of CCh required to evoke the effects above suggested that CCh might, in fact, be acting on nicotinic receptors. This was confirmed as pre-exposure of preparations to the nicotinic receptor antagonist Hex (100 μM for 30 min, n = 6) completely abolished the actions of CCh (Figure 1Bi–iii). Not only did nicotine (100 μM, n = 5) evoke a similar transient decrease in contraction frequency associated with a delayed positive inotropic effect as CCh (Figure 2Ai), it also prevented the action of a subsequent application of CCh (100 μM, n = 3, data not shown).

Effects of capsaicin

It is likely that the nicotinic receptors stimulated above are located on pre-synaptic terminals of the intramural innervation. As we have previously demonstrated that the negative chronotropic and positive inotropic effects of transmural electrical nerve stimulation of the mouse (Hashitani *et al.*, 2009) and guinea pig (Teele and Lang, 1998) renal pelvis are readily mimicked upon the stimulation of transient receptor potential channel subfamily V1 receptors with capsaicin (Hashitani *et al.*, 2009), we investigated whether depletion of neuropeptide from PSAs could prevent the effects evoked upon nicotinic receptor activation. Figure 2Aii illustrates that capsaicin (10 μM for 10 min, n = 13) both mimicked the effects of nicotinic receptor activation (Figure 2Ai–ii) and prevented the action of nicotine (100 μM, Figure 2Aiii, Bi, n = 4) or CCh (100 μM, Figure 2Bii, n = 5) for some 30 min after washout.

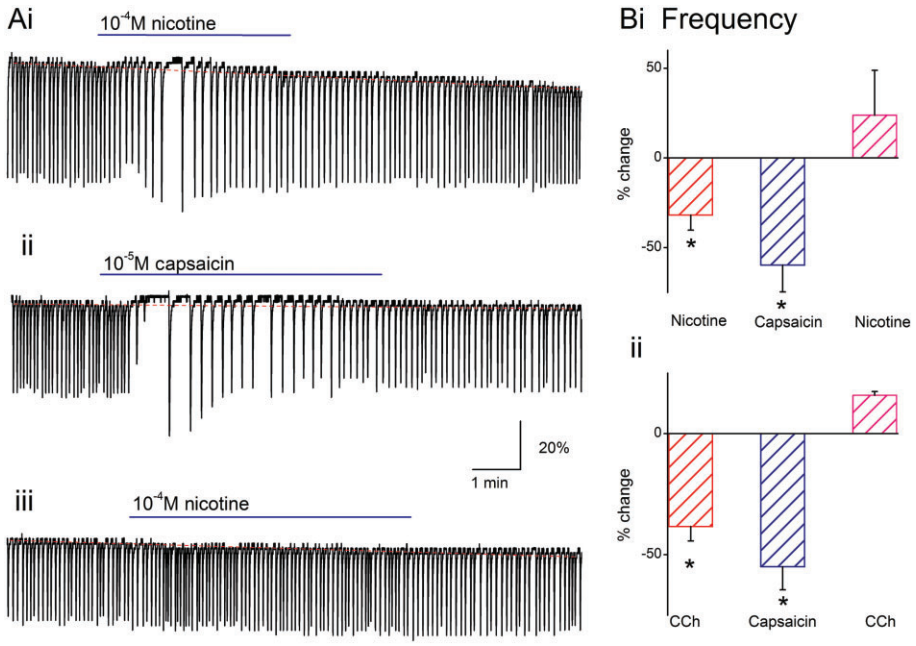

Figure 2

Effects of depleting PSA neuropeptides of their neuropeptides upon stimulation of transient receptor potential channel subfamily V1 receptors with capsaicin. Capsaicin both mimics the negative chronotropic effects of nicotinic receptor activation and prevents the effects evoked by their subsequent activation by nicotine (100 μM) or CCh (100 μM). A Effects of nicotine (100 μM) applied before (Ai) and after (Aiii) an exposure to capsaicin (10 μM) (Aii). All three traces obtained from the same preparation, scale bar applies to all. (B) Summary of the effects of capsaicin (10 nM for 5 min) preventing the negative chronotropic effects of nicotine (100 μM, $n = 4$) (Bi) or CCh (100 μM, $n = 5$) (Bii). Results have been expressed as the mean % change ± SE from the control frequency; * represents a significant difference from zero.

Role of plasmalemmal KATP channels in nicotinic receptor-mediated effects

The negative chronotropic effects evoked upon electrical or capsaicin stimulation of PSAs have been shown to be mimicked by human CGRP (hCGRP) and stimulators of TSMC levels of cAMP, which evoke the opening of Glib-sensitive KATP channels (Maggi *et al.*, 1992; Zhang *et al.*, 1994a; Santicioli and Maggi, 1998; Hashitani *et al.*, 2009).

Ten minute pre-exposure of preparations to 1 μM Glib significantly increased the frequency of the spontaneous contractions of the renal pelvis (to 18.6 ± 6.4, c.f. 11.4 ± 1.5 min^{-1} in control $P < 0.05$, $n = 5$). However, Glib readily prevented the negative chronotropic effects of CCh (100 μM, Figure 3Ai–iii, $n = 4$). Conversely, Glib (1 μM, $n = 5$) applied at the peak of the negative chronotropic effects of CCh (100 μM) readily restored contraction frequency to values above control (i.e. mean frequency in control was 6.03 ± 1.23, in CCh 4.7 ± 1.1 and CCh + Glib 11.0 ± 0.6 min^{-1} respectively; data not shown).

The likely presence of KATP channels on TSMCs was also confirmed by the direct demonstration of a negative chronotropic effect in the renal pelvis in the presence of KATP channels opener, PCO400 (1 μM, $n = 4$), and its reversal upon the addition of Glib (1 μM, $n = 3$, Figure 3B).

Role of plasmalemmal KATP channels on CCh-evoked reduction of action potential frequency

Intracellular microelectrode recordings have previously demonstrated that high-frequency STDs are recorded in ASMCs within the proximal renal pelvis while regenerative action potentials, which can propagate the length of the renal pelvis, are recorded in TSMCs within the pelvis wall (Lang *et al.*, 2007a). We have postulated that this STD discharge in the proximal renal pelvis provides the pacemaker signal that triggers the propagating action potentials, which precede the peristaltic contractions (Lang *et al.*, 2007a,b). In the present experiments, CCh (<10 μM, $n = 4$) had little effect on STD discharge or the action potentials recorded in TSMCs (data not shown). However, at a higher concentration, CCh (100 μM, $n = 8$) significantly reduced STD and action potential discharge (Figure 4Ai–ii), but increased the half width of the action potentials recorded in TSMCs (Table 2). These negative chronotropic effects were accompanied by a significant membrane hyperpolarization of 5.8 ± 4.7 mV ($n = 6$ significantly different from zero $P < 0.05$; Figure 4Aii–iii, Bi).

Similar membrane hyperpolarizations and negative chronotropic and positive inotropic effects on action potential discharge in the renal pelvis have previously been observed with hCGRP and agents that raise intracellular levels of cAMP: iosprenaline, forskolin, 8-bromo-cAMP (Hashitani *et al.*, 2009) and caffeine (Lang *et al.*, 2006).

In preparations pretreated with Glib (10 μM for 10 min, $n = 4$), CCh (100 μM) failed to hyperpolarize the membrane potential (Figure 4Bi-ii) but still reduced the frequency of spontaneous action potentials discharge. The effects of Glib were reversibly upon washout (Figure 4Biii). In contrast, the positive inotropic and negative chronotropic effects of CCh (100 μM) were not prevented by iberiotoxin (100 nM for 10 min, $n = 3$), the selective blocker of large conductance

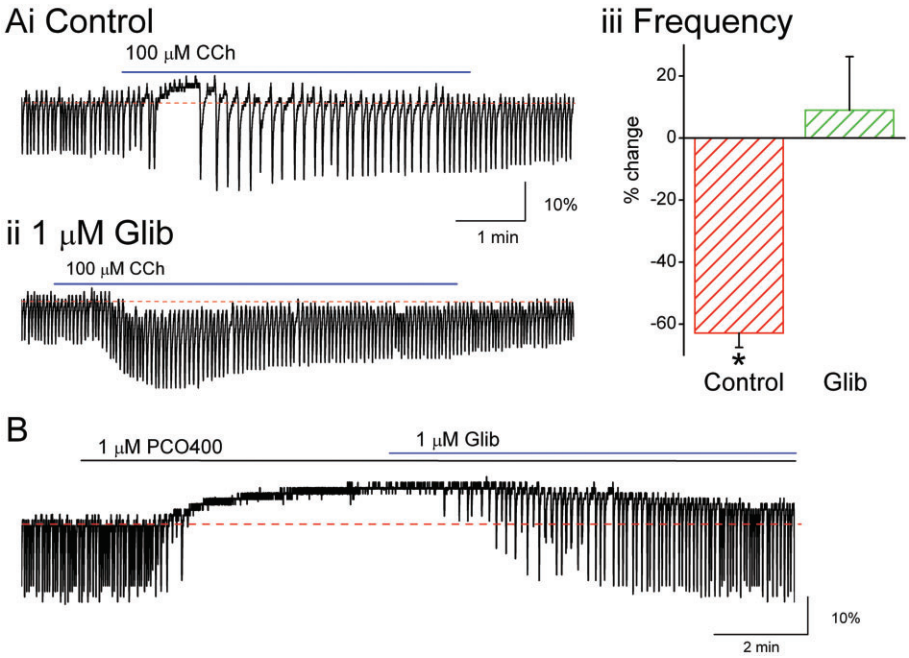

Figure 3

Effects of blocking KATP channels on the inhibitory effects on renal pelvis contractility evoked by CCh or the KATP channel opener PCO400. (Ai–ii) Typical example of the effects of Glib (1 μM) preventing the negative chronotropic effects of CCh (100 μM), scale bar refers to both traces. (Aiii) Summary of the effects of Glib (1 μM for 10 min) preventing the negative chronotropic effects of CCh (100 μM, $n = 5$). Results have been expressed as the mean % change from the control frequency; * represents a significant difference from zero. (B) The inhibition of the renal pelvis contractility by the cromakalim analogue PCO400 (1 μM, $n = 5$) was readily reversed by Glib (1 μM, $n = 4$).

Table 2

Effects of CCh (100 μM) on the parameters of spontaneous action potentials and Ca^{2+} transients in TSMCs of the mouse renal pelvis

	Amplitude	1/2 width	Frequency	*n*
Action potentials	mV	ms	min^{-1}	
Control	46.7 ± 4.4	1456 ± 237	5.4 ± 1.7	8
CCh	46 ± 2.9	2391 ± 528[a]	1.7 ± 0.5[a]	
Ca^{2+} transients	F_t/F_0	ms	min^{-1}	
Control	0.6 ± 0.1	653 ± 26	17.4 ± 1.9	8
CCh	0.6 ± 0.07	790 ± 35[a]	7.8 ± 1.2[a]	

Data shown as mean ± SE.
[a]Significantly different from control values ($P < 0.05$).

Ca^{2+}-activated K^+ channels, although iberiotoxin evoked a membrane depolarization of some 3–5 mV (data not shown).

Effects of CCh on Ca^{2+} transients in TSMCs and ASMCs

Regular transient rises in $[Ca^{2+}]_i$ (Ca^{2+} transients) were readily recorded in TSMCs within the renal pelvis wall with Fluo-4 (Lang *et al.*, 2007a,b; Figure 5A). In 13 preparations, these transients had a mean amplitude, half width and integral of 0.79 ± 0.08 F_t/F_0, 679.9 ± 59.3 ms, 4780 ± 558 F_t/F_0 ms^{-1}, respectively, and occurred at a frequency of 14.7 ± 1.7 min^{-1}.

The effects of CCh (100 μM) on TSMC Ca^{2+} transients recorded in eight preparations are summarized in Table 2. It can be seen that CCh significantly reduced the frequency of these Ca^{2+} transients and this negative chronotropic effect was associated with a significant increase in their 1/2 width, little change in their amplitude and a significant fall in the baseline fluorescence of –0.11 ± 0.08 F_0/F_t (significantly different from zero $P < 0.05$; Figure 5B).

When the same preparations were treated with Glib (10 μM for 10 min), TSMC Ca^{2+} transients had a mean amplitude, half width and frequency of 0.61 ± 0.05 F_t/F_0, 397 ± 50 ms, and 17.4 ± 1.9 min^{-1}, respectively (c.f. 0.64 ± 0.07

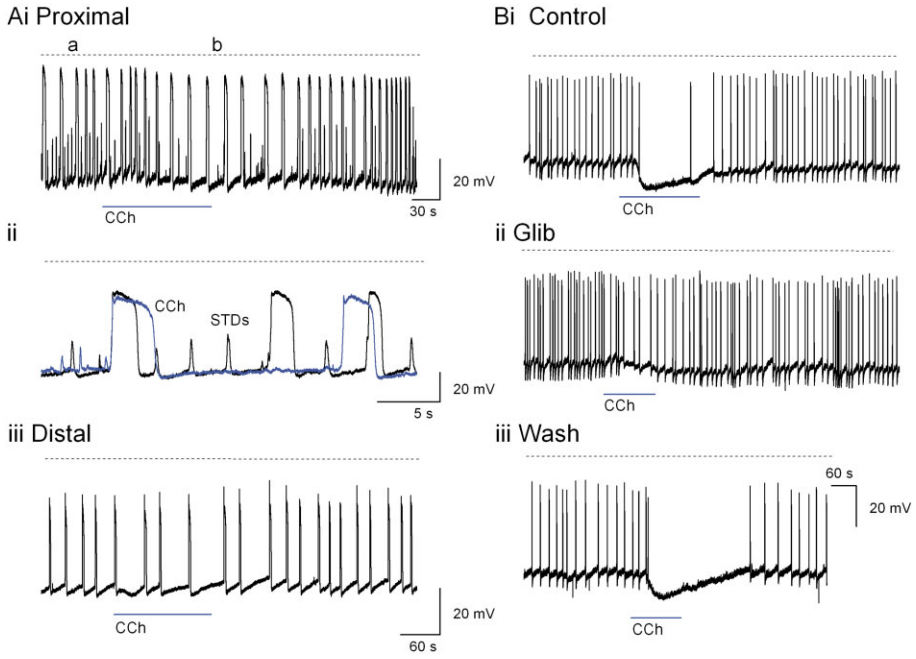

Figure 4

Blockade of KATP channels reduces the negative chronotropic effects of nicotinic receptor activation on the spontaneous action potentials recorded in TSMCs of the mouse renal pelvis. CCh (100 μM) caused a membrane hyperpolarization and a decrease in the frequency of action potential discharge in both the proximal (Ai–ii) and distal (Aiii) renal pelvis. This decrease was associated with a significant increase in the half amplitude duration of recorded action potentials and a reduction the frequency of STD discharge. (Aii) Sections of trace in Ai indicated by a and b were superimposed and displayed on an expanded time base. Dashed lines represents 0 mV. (B) Glib (10 μM for 10 min) blocked the membrane hyperpolarization (Bi–ii) and reduced but did not abolish the negative chronotropic effect of CCh (100 μM, $n = 6$). The inhibitory effects of Glib were readily reversible (Biii). Scale bar applied to all three traces, dashed lines represent 0 mV.

F_t/F_0 ($P > 0.05$), 654 ± 26 ms ($P < 0.05$) and 16.4 ± 1.5 min^{-1} ($P > 0.05$) in control). Glib prevented the CCh (100 μM) reduction in discharge frequency (16.4 ± 1.5 min^{-1}, $P > 0.05$) and significantly reduced the change in baseline (0.01 ± 0.03 F_t/F_0 c.f. with control above $P < 0.05$; Figure 5C,D). However, CCh still significantly increased the 1/2 width of the Ca^{2+} transients to 667 ± 40 ms ($P < 0.05$) in Glib (Figure 5D).

Effects of CCh on ASMC Ca^{2+} transients were best observed after suppression of all action potential discharge and contractility with 3 μM nifedipine (Lang *et al.*, 2007a,b; Figure 6A). 306 Ca^{2+} transients in 26 ASMCs ($n = 26$ cells, $n = 6$ preparations) had a mean amplitude, half width, integral and frequency of 0.47 ± 0.04 F_t/F_0, 840.7 ± 39 ms, 423.5 ± 39 F_t/F_0 $ms^{-1}$and 9.97 ± 2.1 min^{-1} respectively (Figure 6). Application of CCh (100 μM for 4–6 min) evoked a transient (1–2 min) inhibition of Ca^{2+} transient discharge that was associated with a significant reduction in the resting Ca^{2+} levels of –0.12 ± 0.01 F_t/F_0 ($n = 27$ cells, $n = 7$ $P < 0.05$).

The effects of capsaicin on this CCh-evoked inhibition of ASMC activity were investigated in 12 cells in three preparations (Figure 6Bi–iii). Before capsaicin treatment, Ca^{2+} transients had a mean amplitude, half width, integral and frequency of 0.34 ± 0.04 F_t/F_0, 591.5 ± 40.3 ms, 224 ± 41 F_t/F_0 ms^{-1} and 10.9 ± 0.9 min^{-1} respectively. Application of capsaicin (10 μM) evoked a strong sustained inhibition of all Ca^{2+} transients recorded in ASMCs (Figure 6Bii). After 10–15 min washout, their mean amplitude, 1/2 width and integral were still reduced, being 0.21 ± 0.02 F_t/F_0 ($P < 0.05$), 515.9 ± 17.5 ms and 105.5 ± 9.4 F_t/F_0 ms^{-1} ($P < 0.05$) respectively. In contrast, the frequency of Ca^{2+} transient discharge returned to control values (10.6 ± 1.5 min^{-1}) after 10–15 min washout. CCh (100 μM) applied after this washout of capsaicin had little effect on the spontaneous Ca^{2+} transients recorded in ASMCs (Figure 6Aiii, $n = 12$, $n = 3$).

In contrast, pretreatment of preparations with Glib (10 μM for 10 min, $n = 3$) had little effect on the negative chronotropic and inotropic effects of CCh (100 μM) on ASMC Ca^{2+} transients. Indeed, it appeared that the effects of CCh were more prolonged in Glib (Figure 6Ci–ii).

Effects of the non-selective COX inhibitor Indo

Sensory nerves within the upper urinary tract have long been thought to play both an afferent and efferent role in controlling the movement of urine from the kidney to bladder (Davidson and Lang, 2000; Lang *et al.*, 2002; Thulesius and Angelo-Khattar, 1985; Zhang and Lang, 1994b). Distension in one renal pelvis induces an increase in afferent renal nerve activity in the ipsilateral kidney as well as in the efferent renal nerves of the contralateral kidney to increase urinary flow, both effects involving the synthesis and release of PGs (Kopp and Smith, 1991). Application of selective COX inhibitors has demonstrated that COX1 is the primary synthesizer of PGs in the rat renal pelvis, while COX2 was the predominately active enzyme in the guinea pig (Davidson and Lang, 2000).

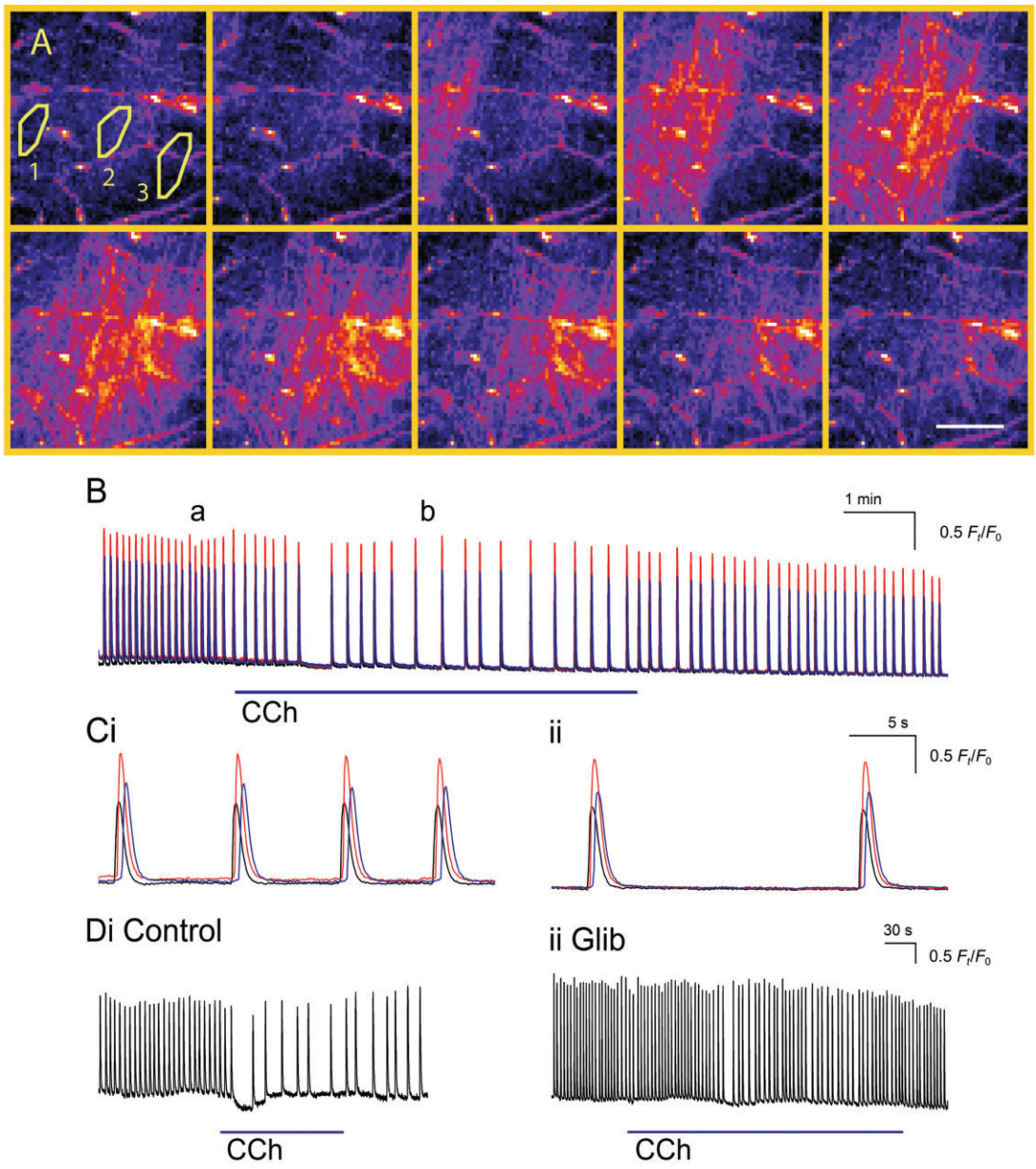

Figure 5

Blockade of KATP channels reduces the negative chronotropic effects of nicotinic receptor activation on the spontaneous Ca^{2+} transients recorded in TSMCs. A sequential Ca^{2+} fluorescence micrographs of Fluo-4-loaded TSMC layer with time intervals of 100 ms observed at ×20 magnification, scale bar represents 100 μm. A Ca^{2+} wave can be clearly seen to as a transient increase in fluorescence intensity sweeping across the field of view. Regions of interest 1, 2 and 3 represented in B by black, red and blue lines respectively. (B) Typical example of the effects of CCh (100 μM, $n = 13$) on the spontaneous Ca^{2+} transients recorded in TSMCs. Coloured traces represent three points within the field of view to indicate direction and velocity of the propagating Ca^{2+} waves. (Ci–ii) Sections of trace in B indicated by a and b, respectively, were superimposed and displayed on an expanded time base. (D) The effects of CCh (100 μM) on the frequency of TSMC Ca^{2+} transients were reduced by Glib (10 μM for 10 min, $n = 7$). Changes in $[Ca^{2+}]_i$ were expressed as the ratio (F_t/F_0) of the fluorescence generated at time t (F_t) and the initial baseline fluorescence at $t = 0$ (F_0).

Figure 7Aii,iv illustrates that Indo (10 and 20 μM for 20 min, $n = 6$) decreased the contraction frequency in a concentration-dependent manner and that the excitatory agonist, Dino (10 nM Figure 7Ai), reversed this effect of Indo (Figure 7Aiii). Moreover, the negative chronotropic and inotropic effects of Indo (20 μM; Figure 7Bii) were still evident in the presence of Glib (1 μM, $n = 5$; Figure 7Bi–ii).

Discussion

In the mouse or guinea pig renal pelvis, stimulation of PSAs with direct repetitive electrical stimulation or capsaicin causes the release of both excitatory and inhibitory neuropeptides that modulate pyeloureteric peristalsis. The relative strength and duration of these negative chronotropic and

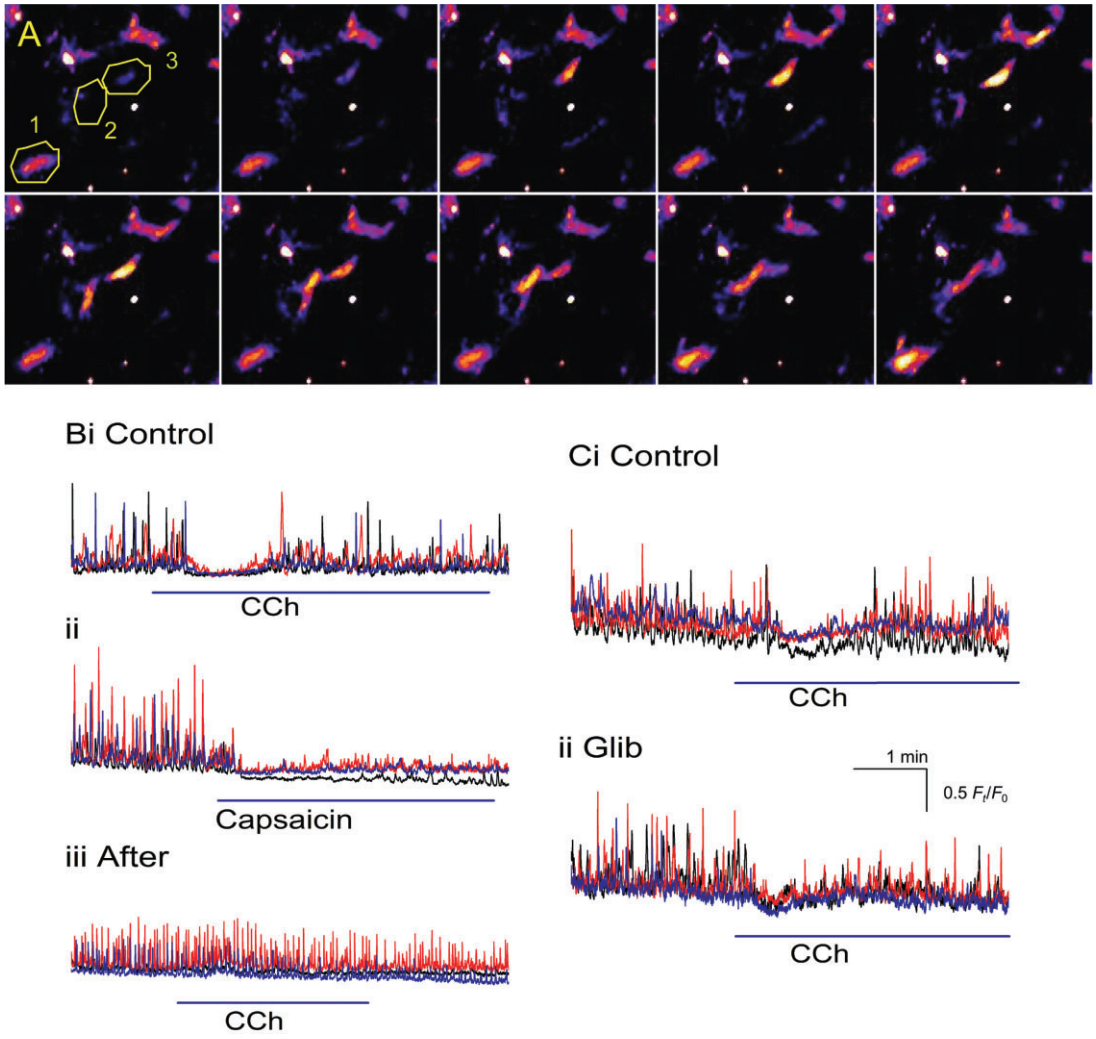

Figure 6

Comparison of the effects of capsaicin and Glib on the Ca^{2+} transients recorded in ASMCs. A sequential coloured Ca^{2+} fluorescence micrographs of Fluo-4-loaded ASMCs with time intervals of 100 ms, observed at ×60 magnification, scale bar represents 30 μm. Regions of interest 1, 2 and 3 represented in Bii by black, blue and red lines respectively. (Bi) Typical example of the transient inhibitory effects of CCh (100 μM) on the spontaneous Ca^{2+} transients recorded in 3 ASMCs bathed in 3 μM nifedipine. In comparison, the inhibitory action of capsaicin (10 μM) was far more prolonged (Bii). (Biii) After 10 min washout of capsaicin, while the frequency of Ca^{2+} transients returned to control values, their amplitude, 1/2 width and integral remained significantly smaller. The negative and inotropic effects of nicotinic receptor activation were also still inhibited. (Ci–ii) The negative chronotropic and inotropic effects of CCh (100 μM) were little affected by pretreatment with Glib (10 μM for 10 min, $n = 3$ 12 cells). Changes in $[Ca^{2+}]_i$ in 3 ASMCs were expressed as the ratio (F_t/F_0) of the fluorescence generated at time t (F_t) and the initial baseline fluorescence at $t = 0$ (F_0). Scale bar applies to all traces.

positive inotropic effects vary in a species-, time- and region-dependent manner (Teele and Lang, 1998; Hashitani *et al.*, 2009). For example, in the guinea pig renal pelvis, the positive inotropic effects of PSA stimulation is robust and occurs before a sustained negative inotropic effect in the proximal regions, but is mostly absent in the distal regions (Teele and Lang, 1998). In the mouse renal pelvis, the positive inotropic effects of PSA stimulation are evident during the time course of the negative chronotropic effects (Figure 2Aii; Hashitani *et al.*, 2009). The negative chronotropic effects of PSA stimulation are mimicked by bath-applied hCGRP and reduced with the CGRP receptor antagonist hCGRP(8–37) (Maggi *et al.*, 1992; Hashitani *et al.*, 2009), again with the guinea pig distal renal pelvis being more sensitive than the proximal regons (Teele and Lang, 1998).

In the guinea pig renal pelvis, the robust positive inotropic effect of PSA stimulation has been attributed to the release of excitatory neuropeptides, neurokinin A and to a lesser extent substance P, as they are largely blocked by MEN 10376, the neurokinin A antagonist (Maggi *et al.*, 1992; Santicioli and Maggi, 1998). In contrast, the positive inotropic effects of PSA stimulation on the mouse renal pelvis have mainly been attributed to the presence of longer duration action potentials and Ca^{2+} transients in TSMCs arising from an accelerated uptake and enhanced release of Ca^{2+} into mitochondria and the sarcoplasmic reticulum as

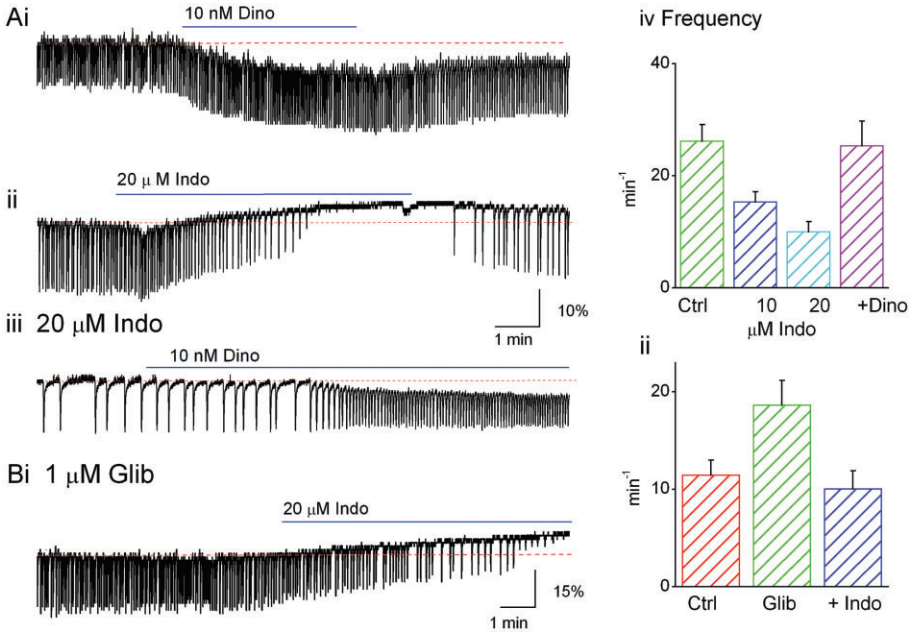

Figure 7

The negative chronotropic and inotropic effects of COX inhibition with Indo occur independently of KATP channels. (Ai) Dino (10 nM, $n = 6$), the PGF2α analogue, evokes a positive chronotropic effect on the frequency of contraction. (Aii,iv) Indo (10 and 20 μM, $n = 6$) produces a concentration-dependent decrease in the frequency of the spontaneous contractions in the renal pelvis, which was readily reversed upon the addition of Dino (10 nM, $n = 6$) (Aii–iii). (Bi) Unlike nicotinic receptor activation, the negative chronotropic and inotropic effects of Indo (20 μM) were not prevented by pretreatment with Glib (1 μM). (Bii) Summary of the effects of Glib (1 μM, $n = 5$) and the addition of Indo (20 μM) on the frequency of contractions in the renal pelvis.

the frequency of discharge is reduced (Hashitani *et al.*, 2009).

In the present experiments, the negative chronotropic and positive inotropic effects evoked by high concentrations of CCh on the spontaneous contractions were unaffected by muscarinic antagonists, but were prevented by Hex or depletion of PSA neuropeptides with capsaicin. These data suggest that there are relatively few functional Ms on either ASMCs or TSMCs, be they M2 that would lead to G_i protein-coupled inhibition of adenylyl cyclase and decrease in cAMP, or M3 that evoke increases in phosphatidylinositol metabolism via a $G_{q/11}$ protein activation of PLC-β and an IP_3-dependent release of Ca^{2+} from internal stores (Wheeler *et al.*, 1995). Instead, our data suggest that the nicotinic receptors located on PSAs within the renal pelvis wall are being activated in the present experiments (Figure 8). Single transmural electrical nerve stimulation invariably fails to influence the spontaneous contractility in the renal pelvis in many species (Maggi *et al.*, 1992; Santicioli and Maggi, 1998), suggesting that neither sympathetic nor parasympathetic nerves form any functioning 'junctional neurotransmission' with the ASMCs or TSMCs within the renal pelvis. However, the presence of these presynaptic nicotinic receptors on neighbouring PSAs provides a novel mechanism by which parasympathetic nerve-released ACh can modulate pyeloureteric peristalsis. This mechanism perhaps mirrors the modulation of PSA function by ACh, ATP and NO released by the urothelium or efferent nerves in response to bladder filling (Kullmann *et al.*, 2008; Sellers and Chess-Williams, 2012).

The presence of PSA nicotinic receptors is consistent and might explain the often unimpressive and contradictory effects of cholinergic agonists on the contractility of the upper urinary tract. Cholinergic agents increase the basal tone and phasic contractions of the renal pelvis of the pig (Sorensen *et al.*, 1983) and guinea pig (Santicioli and Maggi, 1998) and the pig intravesical ureter (Hernandez *et al.*, 1993), but have little effect on contractility of human ureter (Tomiak *et al.*, 1985), rat renal pelvis (Finberg and Peart, 1970) or peristalsis in the ureter of conscious pigs (Roshani *et al.*, 2003).

Glib (10 μM) blocked the membrane hyperpolarization of TSMCs to bath-applied CCh (Figure 4), as well as to CGRP or stimulants of cAMP levels such as IBMX, forskolin (Hashitani *et al.*, 2009) and caffeine (Lang *et al.*, 2006). In the present experiments, Glib (1 μM) partially reversed the negative chronotropic effects of CCh on TSMC contractility (Figure 3) and their underlying action potentials (Figure 4) and Ca^{2+} transients (Figure 5). However, Glib did not affect the CCh-evolved negative chronotropic effects on ASMC Ca^{2+} transients (Figure 6). These data support our earlier suggestion that TSMC may selectively express KATP channels and that the frequency of action potential generation is voltage independent, driven by neighbouring pacemaker mechanisms located in ASMCs (Hashitani *et al.*, 2009; Figure 8).

As capsaicin prevented the inhibition of ASMCs Ca^{2+} transient discharge upon nicotinic receptor stimulation (Figure 6), these negative inotropic and chronotropic effects can again be attributed to PSA release of CGRP. Previously, we

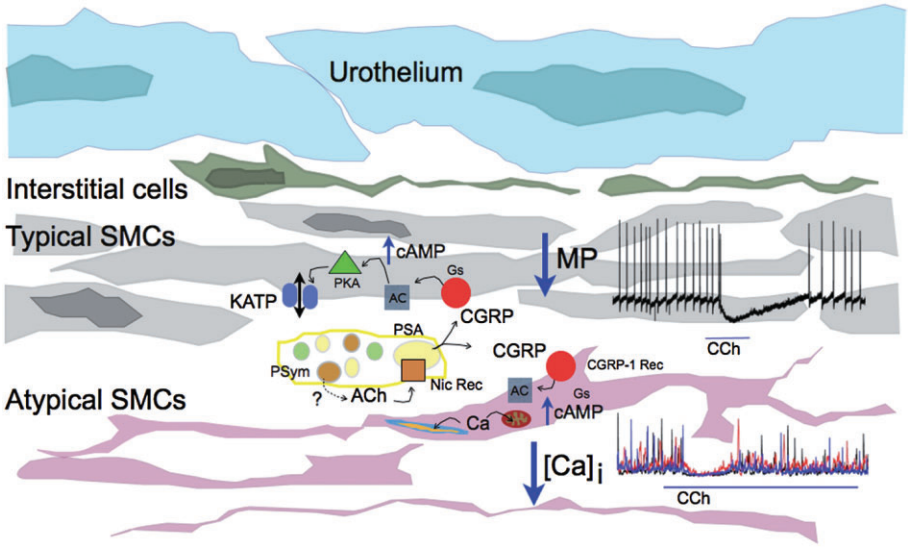

Figure 8

Summary of the mechanisms by which the parasympathetic innervation may influence pyeloureteric peristalsis. We suggest that Ach released from parasympathetic (Psym) nerves activate nicotinic receptors on neighbouring PSAs, which in turn transiently releases CGRP. This CGRP binds to its GPCR (CGRP receptor subfamily 1) on both ASMCs and TSMCs to evoke a rise in intracellular cAMP. In ASMCs, this rise in cAMP promotes an increase in the Ca^{2+}-buffering capacity of both mitochondria and endoplasmic reticulum stores, which reduces the intracellular cycling of Ca^{2+}. This leads to an inhibition of the ASMC Ca^{2+} transients as well as a fall in the resting $[Ca^{2+}]_i$ resulting in a decreased pacemaker drive arising from the proximal renal pelvis and the observed decrease in frequency of the contractions, action potentials and Ca^{2+} transients in the TSMCs. In contrast, the rise in cAMP in TSMCs leads to the opening of Glib-sensitive KATP channels. The resulting membrane hyperpolarization promotes the de-inactivation of plasmalemmal Ca^{2+} channels in TSMCs. Thus, when a STD arising from a neighbouring ASMC triggers an excitatory response in a TSMC, the resulting action potential and Ca^{2+} transient may well be larger and longer than those observed in control.

have demonstrated that the negative chronotropic and inotropic effects of bath-applied CGRP can be antagonized by the SQ22536, a membrane permeable adenylate cyclase inhibitor and mimcked by forskolin or 8-bromo-cAMP, stimulators of intracellular levels of cAMP and by blockers of mitochondrial function (Hashitani *et al.*, 2009). We envisage that CGRP-evoked rises in cAMP trigger changes in the buffering capacity and mobilization of Ca^{2+} into and out of both mitochondria and the sarcoplasmic reteculum within ASMCs. The sustained decrease in ASMC Ca^{2+} transients after exposure to capsaicin may also suggests that a tonic release of PSA tackykinins maintains normal ASMC activity (Lang, 2010). The relative effects of PSA-released tachykinins and CGRP appear very species dependent, capsacin elciciting a robust positive inotropic response in the guinea pig renal pelvis (Teele and Lang, 1998), but only a short transient response in the mouse (Hashitani *et al.*, 2009).

In summary, the negative chronotropic and positive inotropic effects of nicotinic receptor activation in the mouse renal pelvis appears to recruit the same cAMP-dependent inhibitory mechanisms recruited by nerve-released or bath-applied CGRP. In TSMCs, these effects involve, in part, membrane hyperpolarization arising from the activation of KATP channels. In contrast, the mechanisms underlying the negative inotropic effects of CCh in ASMCs have yet to be fully established but are likely to involve an increase in Ca^{2+} buffering by the mitochondria and endoplasmic reticulum stores, resulting in a reduction in the intracellular cycling of Ca^{2+}. Given the relative insensitivity of the upper urinary tract to muscarinic agonists or transmural electrical stimulation (Maggi *et al.*, 1992; Santicioli and Maggi, 1998), pre-synaptic nicotinic receptors on PSAs may well provide the means by which neighbouring parasympathetic nerves modulate pyeloureteric peristalsis, such a mechanism being analogous to the modulation of bladder PSAs by efferent nerve- and urothelium-derived factors.

Acknowledgements

This work was supported by the Japanese Society for the Promotion of Science (to H. H.) and in part by the National Health and Medical Research Council (Australia) (to R. L.).

Conflict of interest

The authors state no conflict of interest.

References

Alexander SP, Mathie A, Peters JA (2011). Guide to Receptors and Channels (GRAC), 5th edn. Br J Pharmacol 164 (Suppl. 1): S1–S324.

Davidson ME, Lang RJ (2000). Effects of selective inhibitors of cyclo-oxygenase-1 (COX-1) and cyclo- oxygenase-2 (COX-2) on the

spontaneous myogenic contractions in the upper urinary tract of the guinea-pig and rat. Br J Pharmacol 129: 661–670.

Finberg JP, Peart WS (1970). Function of smooth muscle of the rat renal pelvis response of the isolated pelvis muscle to angiotensin and some other substances. Br J Pharmacol 39: 373–381.

Golenhofen K, Hannappel J (1973). Normal spontaneous activity of the pyeloureteral system in the guinea-pig. Pflugers Arch 341: 257–270.

Gosling JA, Dixon JS (1974). Species variation in the location of upper urinary tract pacemaker cells. Invest Urol 11: 418–423.

Hashitani H, Lang RJ, Mitsui R, Mabuchi Y, Suzuki H (2009). Distinct effects of CGRP on typical and atypical smooth muscle cells involved in generating spontaneous contractions in the mouse renal pelvis. Br J Pharmacol 158: 2030–2045.

Hernandez M, Simonsen U, Prieto D, Rivera L, Garcia P, Ordaz E *et al*. (1993). Different muscarinic receptor subtypes mediating the phasic activity and basal tone of pig isolated intravesical ureter. Br J Pharmacol 110: 1413–1420.

Kilkenny C, Browne W, Cuthill IC, Emerson M, Altman DG (2010). Animal research: Reporting *in vivo* experiments: The ARRIVE guidelines. Br J Pharmacol 160: 1577–1579.

Klemm MF, Exintaris B, Lang RJ (1999). Identification of the cells underlying pacemaker activity in the guinea- pig upper urinary tract. J Physiol 519: 867–884.

Kopp UC, Smith LA (1991). Inhibitory renorenal reflexes: a role for renal prostaglandins in activation of renal sensory receptors. Am J Physiol 261: R1513–R1521.

Kullmann FA, Artim D, Beckel J, Barrick S, de Groat WC, Birder LA (2008). Heterogeneity of muscarinic receptor-mediated Ca^{2+} responses in cultured urothelial cells from rat. Am J Physiol Renal Physiol 294: F971–F981.

Lang RJ (2010). Role of hyperpolarization-activated cation channels in pyeloureteric peristalsis. Kidney Int 77: 483–485.

Lang RJ, Exintaris B, Teele ME, Harvey J, Klemm MF (1998). Electrical basis of peristalsis in the mammalian upper urinary tract. Clin Exp Pharmacol Physiol 25: 310–321.

Lang RJ, Takano H, Davidson ME, Suzuki H, Klemm MF (2001). Characterization of the spontaneous electrical and contractile activity of smooth muscle cells in the rat upper urinary tract. J Urol 166: 329–334.

Lang RJ, Davidson ME, Exintaris B (2002). Pyeloureteral motility and ureteral peristalsis: essential role of sensory nerves and endogenous prostaglandins. Exp Physiol 87: 129–146.

Lang RJ, Tonta MA, Zoltkowski BZ, Meeker WF, Wendt I, Parkington HC (2006). Pyeloureteric peristalsis: role of atypical smooth muscle cells and interstitial cells of Cajal-like cells as pacemakers. J Physiol 576: 695–705.

Lang RJ, Hashitani H, Tonta MA, Parkington HC, Suzuki H (2007a). Spontaneous electrical and Ca^{2+} signals in typical and atypical smooth muscle cells and interstitial cell of Cajal-like cells of mouse renal pelvis. J Physiol 583: 1049–1068.

Lang RJ, Hashitani H, Tonta MA, Suzuki H, Parkington HC (2007b). Role of Ca^{2+} entry and Ca^{2+} stores in atypical smooth muscle cell autorhythmicity in the mouse renal pelvis. Br J Pharmacol 152: 1248–1259.

Lang RJ, Hashitani H, Tonta MA, Bourke JL, Parkington HC, Suzuki H (2010). Spontaneous electrical and Ca^{2+} signals in the mouse renal pelvis that drive pyeloureteric peristalsis. Clin Exp Pharmacol Physiol 37: 509–515.

McGrath J, Drummond G, McLachlan E, Kilkenny C, Wainwright C (2010). Guidelines for reporting experiments involving animals: the ARRIVE guidelines. Br J Pharmacol 160: 1573–1576.

Maggi CA, Theodorsson E, Santicioli P, Giuliani S (1992). Tachykinins and calcitonin gene-related peptide as co- transmitters in local motor responses produced by sensory nerve activation in the guinea-pig isolated renal pelvis. Neuroscience 46: 549–559.

Rolle U, Brylla E, Tillig B, Chertin B, Cascio S, Puri P (2008). Demonstration of intrinsic innervation of the guinea pig upper urinary tract using whole-mount preparation. Neurourol Urodyn 27: 341–347.

Roshani H, Dabhoiwala NF, Dijkhuis T, Pfaffendorf M, Boon TA, Lamers WH (2003). Pharmacological modulation of ureteral peristalsis in a chronically instrumented conscious pig model. I: effect of cholinergic stimulation and inhibition. J Urol 170: 264–267.

Santicioli P, Maggi CA (1998). Myogenic and neurogenic factors in the control of pyeloureteral motility and ureteral peristalsis. Pharmacol Rev 50: 683–722.

Sellers DJ, Chess-Williams R (2012). Muscarinic agonists and antagonists: effects on the urinary bladder. Handb Exp Pharmacol 208: 375–400.

Sorensen SS, Husted SE, Nissen T, Djurhuus JC (1983). Topographic variations in alpha-adrenergic and cholinergic response in the pig renal pelvis. Urol Int 38: 271–274.

Teele ME, Lang RJ (1998). Stretch-evoked inhibition of spontaneous migrating contractions in a whole mount preparation of the guinea-pig upper urinary tract. Br J Pharmacol 123: 1143–1153.

Thulesius O, Angelo-Khattar M (1985). The effect of indomethacin on the motility of isolated sheep ureters. Acta Pharmacol Toxicol (Copenh) 56: 298–301.

Tomiak RH, Barlow RB, Smith PJ (1985). Are there valid reasons for using anti-muscarinic drugs in the management of renal colic? Br J Urol 57: 498–499.

Weiss R, Wagner ML, Hoffman BF (1967). Localization of the pacemaker for peristalsis in the intact canine ureter. Invest Urol 5: 42–48.

Wheeler MA, Martin TV, Weiss RM (1995). Effect of carbachol and norepinephrine on phosphatidyl-inositol hydrolysis and cyclic-amp levels in guinea-pig urinary-tract. J Urol 153: 2044–2049.

Zhang Y, Lang RJ (1994). Effects of intrinsic prostaglandins on the spontaneous contractile and electrical activity of the proximal renal pelvis of the guinea-pig. Br J Pharmacol 113: 43–48.

Zhang L, Bonev AD, Nelson MT, Mawe GM (1994). Activation of ATP-sensitive potassium currents in guinea-pig gall-bladder smooth muscle by the neuropeptide CGRP. J Physiol 478: 483–491.